

Research Article

Facile Postsynthesis of N-Doped TiO₂-SBA-15 and Its Photocatalytic Activity

Thu Phuong Tran Thi,¹ Duc Trieu Nguyen,¹ Tuan Quang Duong,²
Huy Hoang Luc,³ and Vien Vo¹

¹ Department of Chemistry, Quy Nhon University, Quy Nhon 8456, Vietnam

² Department of Chemistry, Hue University of Education, Hue 8454, Vietnam

³ Department of Physics, Hanoi National University of Education, Ha Noi 844, Vietnam

Correspondence should be addressed to Vien Vo; vovien@qnu.edu.vn

Received 7 May 2013; Accepted 23 July 2013

Academic Editor: Z. Barber

Copyright © 2013 Thu Phuong Tran Thi et al. This is an open access article distributed under the Creative Commons Attribution License, which permits unrestricted use, distribution, and reproduction in any medium, provided the original work is properly cited.

N-doped TiO₂-SBA-15 (denoted as N-TiO₂-SBA-15) material has been successfully synthesized by a two-step procedure. Firstly, TiO₂-SBA-15 was prepared by impregnating tetraisopropyl orthotitanate on SBA-15 and followed by calcination at 550°C. In the second step, TiO₂-SBA-15 was modified by doping nitrogen with the assistance of urea. The resulting material, N-TiO₂-SBA-15, was characterized by XRD, TEM, SEM, N₂ adsorption/desorption at 77 K, DR UV-Vis, and XPS. The results showed that N-TiO₂-SBA-15 material maintains its ordered hexagonal mesostructure and exhibits the absorption of visible region. The photocatalytic activity of N-TiO₂-SBA-15 sample was evaluated by the photodegradation of methylene blue under visible light.

1. Introduction

Heterogeneous photodegradation of organic pollutants with semiconductors has attracted much of the attention of researchers because of its efficiency and promises of economy [1, 2]. Among the semiconductor materials, TiO₂ has been investigated more widely due to its high photocatalytic efficiency, commercial availability, chemical stability, and environmental friendliness [3, 4]. However, its technological application seems to be limited by several factors such as relatively low surface area and the requirement of UV light. In order to overcome these limitations, a number of modifications have been tried.

Many efforts have been made on supporting TiO₂ on porous materials for increasing surface area of TiO₂ [5–7]. Among the various porous materials, SBA-15 silica has attracted great attention as an ideal catalytic support due to its large surface area, adjustable pore size ranging from 5 to 30 nm, ordered frameworks with the wall being in the thickness range of 3.1–6.4 nm, and transparency to UV radiation [8].

Over the past decades, in order to extend the useful spectral range into the visible region, metal-doped TiO₂ photocatalysts were intensively studied. However, metal-doped TiO₂ exhibits several drawbacks: thermal instability, electron trapping by the metal centers, and requirement of more expensive ion-implantation facilities [9, 10]. Recently, it was shown that the narrowing of band gap for TiO₂ can be better obtained by using anionic dopants rather than metal ions. In a breakthrough work, Asahi et al. showed that the substitution of oxygen atoms in TiO₂ by nitrogen atoms leads to the narrowing of the band gap by mixing the N 2p and O 2p states [11]. Since then, many synthetic strategies have been applied for doping of the TiO₂ with various nonmetal atoms such as N [12–25], C [26–29], B [30–33], S [34–37], P [38], F [39, 40], and I [41, 42].

These reports all showed that the doping can bring a significant enhancement for the photocatalytic activity of TiO₂ under visible light. Among the nonmetals, N is the most typical nonmetal dopant and has been intensively investigated so far. There are numerous publications on preparation of N-doped TiO₂ by various methods, including

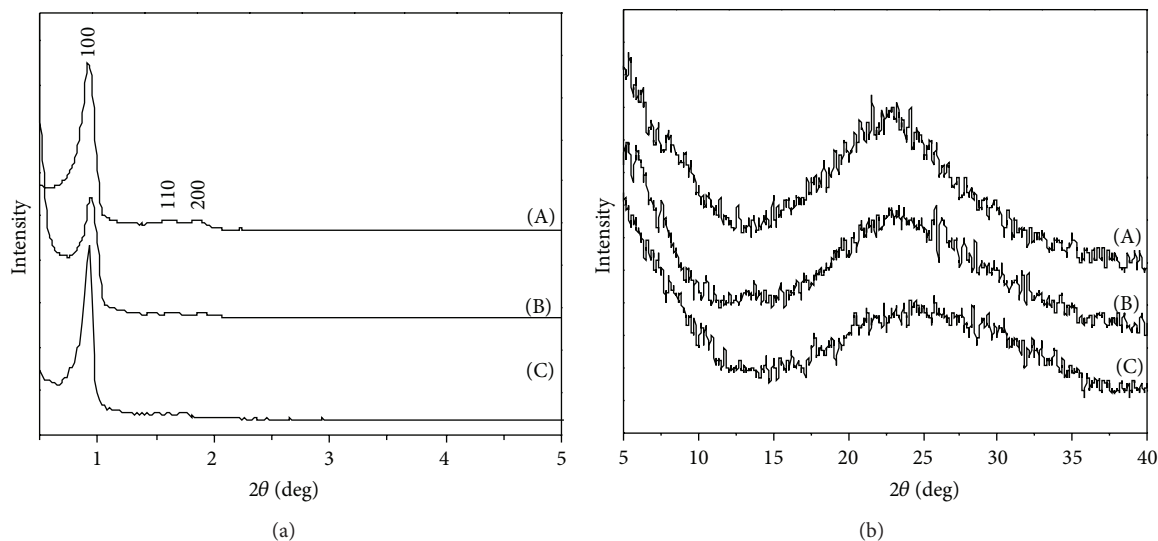


FIGURE 1: (a) Small-angle XRD patterns of the pure SBA-15 (A), TiO₂-SBA-15 (B), and N-TiO₂-SBA-15 (C); (b) Large-angle XRD patterns of the pure SBA-15 (A), TiO₂-SBA-15 (B), and N-TiO₂-SBA-15 (C).

sol-gel [13–20], sputtering [11, 12], ion-implantation [21], and plasma-enhanced chemical vapor deposition [22] methods. Beside NH₃ as a significant nitrogen source for the doping, urea has attracted considered attention as an alternative nitrogen source because of its useful characteristics such as environment-friendly and easy operation in doping [43–45]. The aim of our research study is to use urea as a nitrogen source to synthesize N-doped TiO₂ supported on SBA-15.

A combination of modified TiO₂ and SBA-15 can take advantage of both SBA-15 and TiO₂. In this paper, we report a facile preparation of N-doped TiO₂-SBA-15 using urea as a nitrogen source. The as-synthesized material showed visible-light response and potential application in photodegradation of methylene blue under visible light.

2. Experimental Section

2.1. Chemicals. Triblock copolymer Pluronic P123 (HO(CH₂CH₂O)₂₀(CH₂CH(CH₃)O)₇₀(CH₂CH₂O)₂₀H), tetraethyl orthosilicate (TEOS, (C₂H₅O)₄Si), methylene blue, and titanium isopropoxide (Ti(C₃H₇O)₄) were purchased from Merck. Hydrochloric acid and urea were purchased from Shanghai Chemical Company. All chemicals were used as received without any further purification.

2.2. Synthesis. The mesoporous silica SBA-15 was prepared according to the literature [46]. In a typical synthesis, 2 g of P123 was added to 62.5 g of 1.9 M HCl with stirring. 3.84 g of TEOS was added after the mixture was heated to 40°C. The reaction mixture was stirred for 20 h at 40°C and then aged in an autoclave at 100°C for 24 h. The solid products were separated by filtration and washed with distilled water for several times. The structure directing agent (P123) was removed by heating the samples at 550°C for 6 h in the air. The TiO₂-SBA-15 sample was prepared according to

the following procedure. 0.5 g of SBA-15 was added to the solution of 0.75 g of Ti(C₃H₇O)₄ in 20 mL of ethanol. After evaporation of the solvent with stirring at 40°C, the resulting solid was dried at 100°C for 12 h and then heated at 550°C for 5 h. The obtained solid was denoted as TiO₂-SBA-15. For the doping of TiO₂-SBA-15 with nitrogen, a mixture of TiO₂-SBA-15 and urea solution with the urea/TiO₂-SBA-15 ratio of 1:3 in weight was prepared. After evaporation of the solvent with stirring at 40°C, the resulting solid was dried at 100°C overnight and then calcined at 500°C for 1 h in the air. The resulting material was denoted as N-TiO₂-SBA-15.

2.3. Characterization. X-ray diffraction (XRD) patterns for the samples were measured on a Bruker D8 Advance diffractometer using CuKα radiation (λ = 1.5406 Å). Transmission electron microscopy (TEM) and scanning electron microscopy (SEM) images were recorded on JEOL JEM-2100F and JEOL 5410, respectively. N₂ adsorption-desorption isotherms were obtained on ASAP 2010 at 77 K. Before the measurement, the samples were degassed at 100°C for 6 h. Diffuse-reflectance UV-Vis spectra were investigated on a Sinco S-4100 spectrometer. X-ray photoelectron spectroscopy (XPS) spectra were recorded on a VG Microtech Multilab ESCA 3000 spectrometer.

For the photocatalytic test, 100 mg of the catalyst was suspended in 50 mL of 100 mg/L methylene blue (MB) aqueous solution, and then the mixture was stirred for 2 h in dark to obtain the equilibrium adsorption. The reaction mixture was exposed to visible light from a 300 W lamp with a UV cutoff filter (>420 nm). After a given irradiation time, about 4 mL of the mixture was withdrawn and the catalysts were separated by centrifugation. The selected solutions were measured using a UV-Vis spectrophotometer (Jenway 6800).

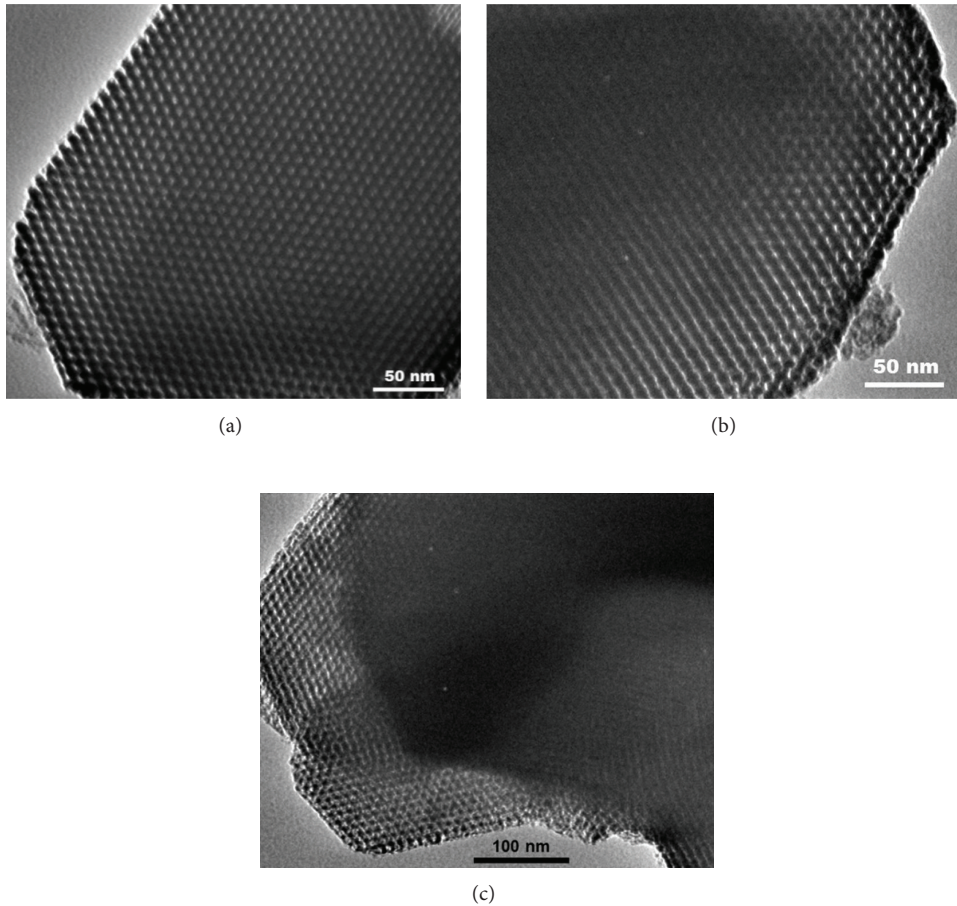


FIGURE 2: TEM images of the pure SBA-15 (a), TiO₂-SBA-15 (b), and N-TiO₂-SBA-15 (c).

3. Results and Discussion

3.1. Characterization of Catalysts. The small-angle X-ray diffraction patterns of pure SBA-15, TiO₂-SBA-15, and N-TiO₂-SBA-15 are shown in Figure 1(a). For the pure SBA-15, three resolved diffraction peaks with 2θ at 0.92°, 1.60°, and 1.84°, indexed as (100), (110), and (200) reflections, are clearly observed, indicative of a two-dimensional hexagonal lattice with high $p6mm$ symmetry [43]. The other materials have an intensive reflection (100), indicating the presence of ordered hexagonal structure similar to the pure SBA-15 silica. However, the peak intensity, especially for (110) and (200) reflections, significantly decreases with the graft of TiO₂ and the doping of nitrogen. This is probably due to decreasing scatter contrast between the silica framework and TiO₂ inside the pores [47, 48]. From the 2θ values of the (100) reflections, the hexagonal lattice parameters are calculated and reported in Table 1.

The large-angle X-ray diffraction for N-TiO₂-SBA-15 was also studied to characterize the structure of TiO₂ grafted on SBA-15 (Figure 1(b)). Also shown are the patterns of SBA-15 and TiO₂-SBA-15. All patterns are similar in shape and show a broad peak centered at about 25° that may be due to amorphous SiO₂ of SBA-15. TiO₂ cannot be detected by

TABLE 1: Structural, textural properties of the pure SBA-15, TiO₂-SBA-15, and N-TiO₂-SBA-15.

Material	S_{BET} (m ² /g)	Pore diameter (nm)	a (nm)	Wall thickness (nm)
SBA-15	689.8	7.5	11.1	3.6
TiO ₂ -SBA-15	529.4	6.6	10.9	4.3
N-TiO ₂ -SBA-15	462.6	6.0	11.1	5.1

XRD, indicating that TiO₂ may disperse homogeneously into nanoparticles on SBA-15.

The periodicity in the mesostructure of the three materials is confirmed directly by transmission electron microscopy (Figure 2). The TEM micrographs display that both the perpendicular and parallel channels relative to the longitudinal axis are observed, which confirms that the modified SBA-15 materials possess ordered, one-dimensional pore structure similar to that of the pure SBA-15. However, a gradual decrease in structural ordering from SBA-15 to TiO₂-SBA-15 to N-TiO₂-SBA-15 can be seen from the images of channels in Figure 2. A raw estimation from the TEM images presents that the pore-pore distances match the lattice parameters calculated from XRD data.

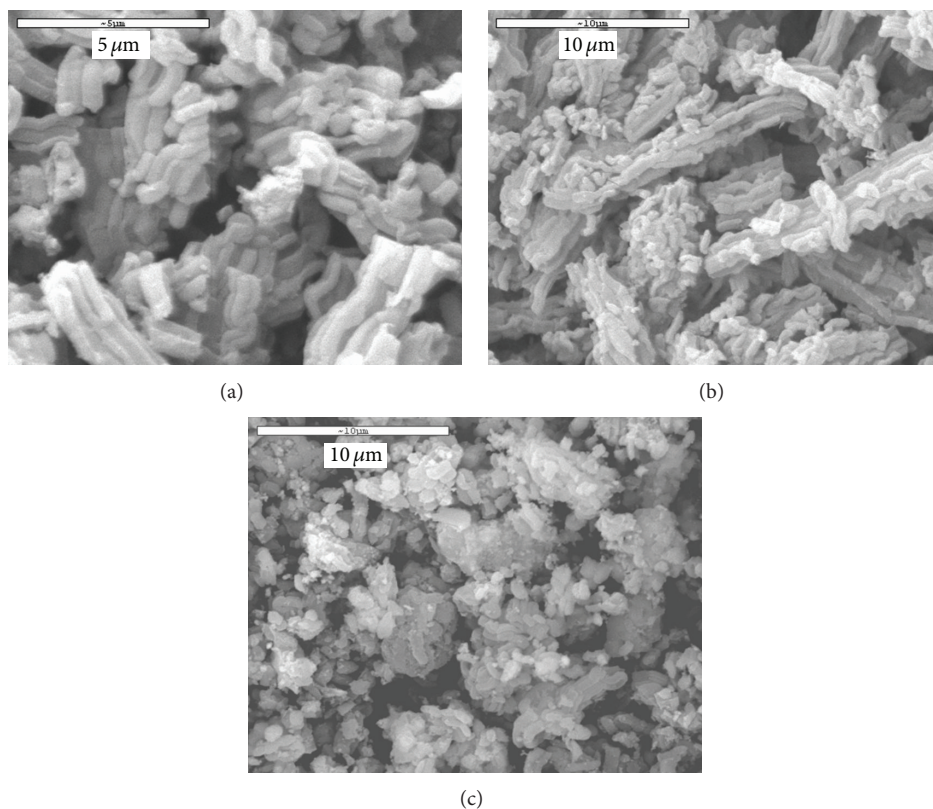


FIGURE 3: SEM images of the pure SBA-15 (a), TiO_2 -SBA-15 (b), and N- TiO_2 -SBA-15 (c).

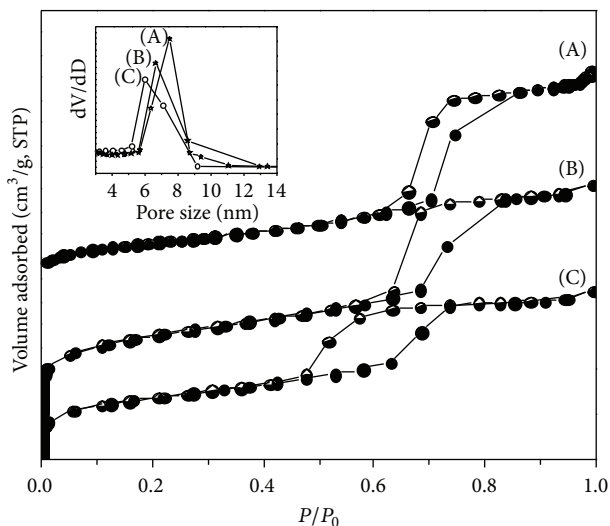


FIGURE 4: N_2 adsorption-desorption isotherms and pore size distribution (the inset) of the pure SBA-15 (A), TiO_2 -SBA-15 (B), and N- TiO_2 -SBA-15 (C).

The morphology of rope-like domains with a uniform size was obtained for the materials SBA-15 and TiO_2 -SBA-15 (Figures 3(a) and 3(b)). A different shape can be seen from Figure 3(c) for N- TiO_2 -SBA-15. The reaction between TiO_2 on SBA-15 and urea may result in breaking the rope-like domains of SBA-15. It can be seen from the TEM and SEM

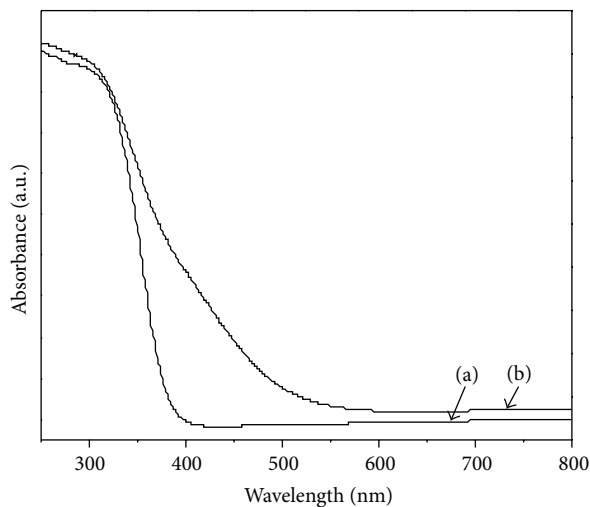


FIGURE 5: Diffuse reflectance UV-Vis spectra of TiO_2 -SBA-15 (a) and N- TiO_2 -SBA-15 (b).

images of TiO_2 -SBA-15 that TiO_2 nanoparticles disperse homogeneously on SBA-15 silica. This is further supported by the large-angle XRD patterns of TiO_2 -SBA-15 without any peaks as mentioned above.

The N_2 adsorption/desorption isotherms at 77 K of the calcined SBA-15 and the modified SBA-15 samples are shown in Figure 4. Type IV IUPAC isotherms, characteristic of

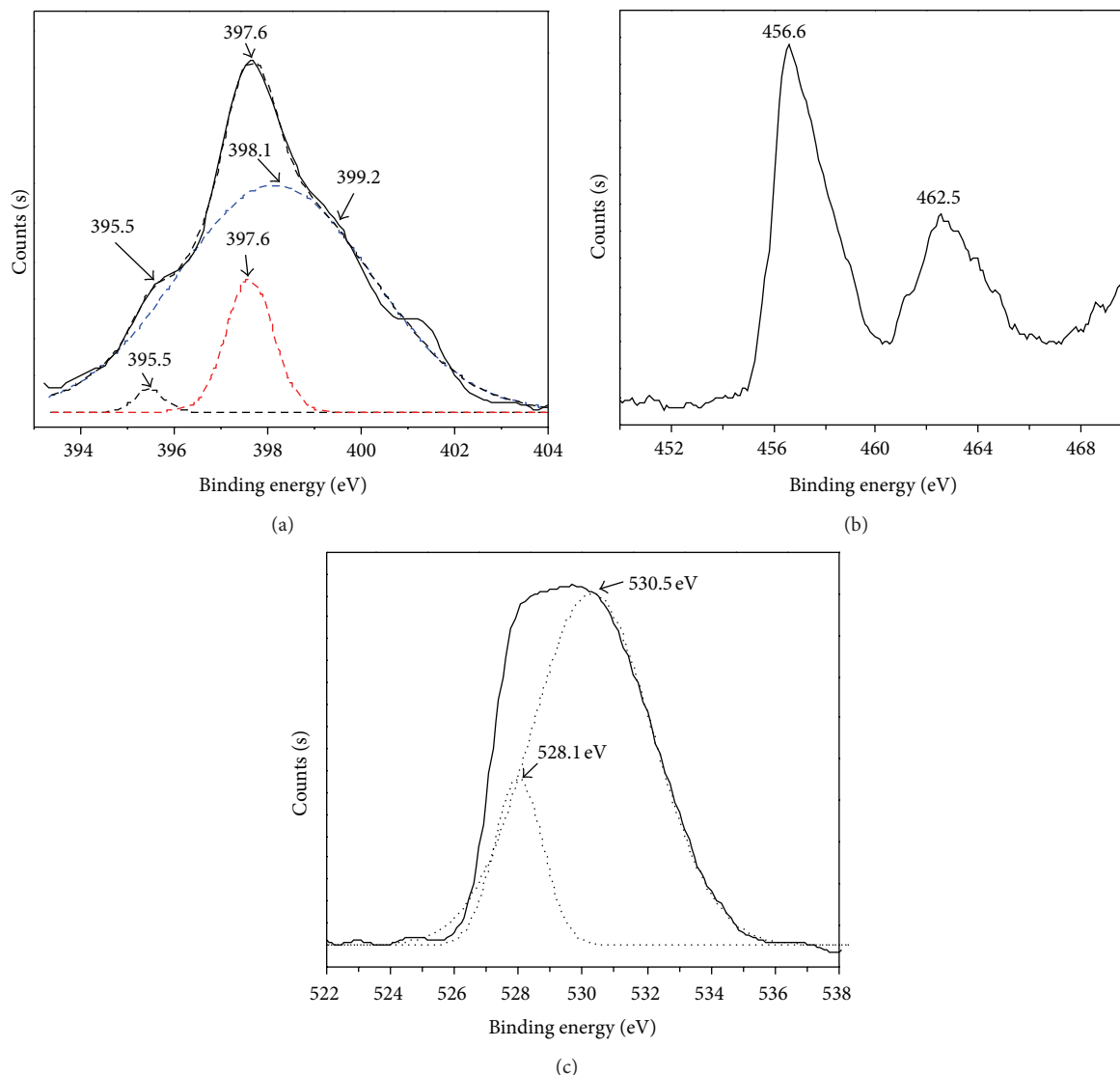


FIGURE 6: XPS spectra of N 1s (a), Ti 2p (b), and O 1s (c) for N-TiO₂-SBA-15.

capillary condensation in mesopores, are found for all samples. However, their shapes are different with a capillary condensation of N₂ occurring over a slightly lower P/P_0 range when going from SBA-15 to TiO₂-SBA-15 to N-TiO₂-SBA-15. The pore-size distribution of the materials is shown in the inset of Figure 4. It can be seen that pore diameters of about 7.5, 6.6, and 6.0 nm for SBA-15, TiO₂-SBA-15, and N-TiO₂-SBA-15, respectively, were obtained. A decrease in specific surface area and pore size was observed in order of the following materials: SBA-15, TiO₂-SBA-15, and N-TiO₂-SBA-15. However, the wall thickness increased in the same order of the materials. These results can be attributed to the fact that TiO₂ particles are attached to the wall of SBA-15 in TiO₂-SBA-15 and some TiO₂ particles are exfoliated from the wall to block the pores in N-TiO₂-SBA-15 when TiO₂-SBA-15 reacted with urea. The summary data on structural, textural properties of the three materials obtained from the N₂ adsorption/desorption isotherms are shown in Table 1.

The doping of TiO₂ on SBA-15 with nitrogen was further supported by the diffuse reflectance UV-Vis spectroscopy. Figure 5 shows that TiO₂-SBA-15 exhibits a strong absorption in UV region corresponding to the band to band transition. Compared with TiO₂-SBA-15, the sample N-TiO₂-SBA-15 possesses a tailing absorption extending out to approximately 600 nm, which is a typical absorption feature of N-doped TiO₂. The absorption in visible light for the sample N-TiO₂-SBA-15 may come from the narrowing band. The band gap value was calculated from the diffuse reflectance measurements to be 2.89 eV.

Chemical states of the doped nitrogen in N-TiO₂-SBA-15 were investigated by XPS. It can be seen from Figure 6(a) that a shape peak around 397.6 eV and two shoulders around 395.5 and 399.2 eV, respectively, for N 1s were found. After fitting the peaks, three peaks at 395.5, 397.6, and 398.1 eV were observed. The binding energy at 395.5 eV can come from replacing the oxygen in the crystal lattice of TiO₂ by nitrogen. The peak

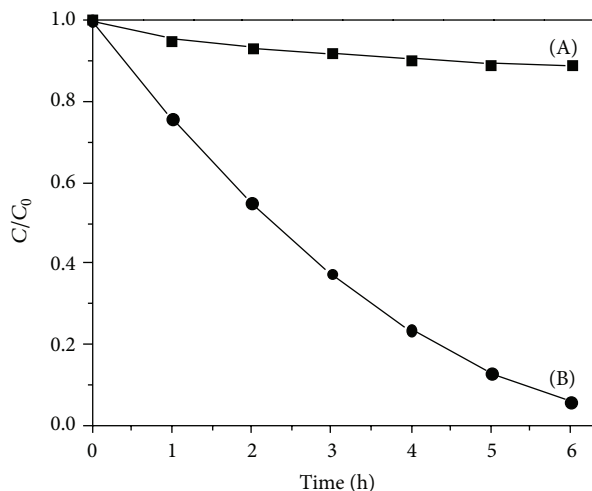


FIGURE 7: Photocatalytic degradation of methylene blue on TiO_2 -SBA-15 (A) and N-TiO_2 -SBA-15 (B) with initial methylene blue concentration of 100 mg/L under visible light.

at 397.6 eV is attributed to the nitrogen anion incorporated in the TiO_2 in N-Ti-O bond. And the strong peak at 398.1 eV can be assigned to the nitrogen in the Ti-O-N site of the N-TiO_2 matrix. These results are consistent with the previous reports [49–51] and will be supported further by the XPS data of Ti 2p and O 1s below. The N content of 3.37% in mol for N-TiO_2 -SBA-15 was obtained from the XPS data.

Compared to Ti-N, a relatively higher binding energy at 397.6 eV for N-Ti-O may be explained by the high electronegativity of oxygen leading to the reduction of electron density on the nitrogen [52]. This is further supported by the result of XPS spectrum for Ti 2p (Figure 6(b)). Two XPS peaks at 456.6 eV and 462.5 eV corresponding to Ti $2p_{3/2}$ and Ti $2p_{1/2}$, respectively, were obtained. The Ti $2p_{2/3}$ peak for pure TiO_2 should be at 458.8 eV [53]. A decrease in the binding energy of Ti $2p_{3/2}$ after nitrogen doping may come from the electronic interaction of Ti with anions in N-TiO_2 , which is different from that of TiO_2 . The lower electronegativity of nitrogen compared to oxygen may lead to a transfer of partial electron from the N to the Ti. Therefore, the electron density around the anion decreases, resulting in the increase in electron density around the cation [54]. This indicates the substitution of oxygen atoms in TiO_2 by nitrogen atoms. The incorporation of nitrogen in TiO_2 can be further confirmed by the binding energy of O 1s. As shown in Figure 6(c), the peak at 530.5 eV may be attributed to the presence of Ti-O-N bonds [52].

3.2. Photocatalytic Test. The photocatalytic activity of the samples was determined by the degradation of methylene blue in water under visible light. Figure 7 shows the variation of methylene blue concentration (C/C_0) with irradiation time over the two catalysts. For the N-TiO_2 -SBA-15 catalyst, it can be seen that the concentration of methylene blue decreases rapidly in the initial three hours and slowly in the later period. Methylene blue can be effectively degraded in the presence of

N-TiO_2 -SBA-15, and the degradation efficiency reaches about 90% in 6 h irradiation. For comparison, the photodegradation of methylene blue for the sample TiO_2 -SBA-15 under the same conditions is also shown in Figure 7. An insignificant catalytic activity of about 3–5% is obtained for the sample without nitrogen doping.

4. Conclusion

The visible-light-sensitive nitrogen-doped TiO_2 -SBA-15 material was synthesized by a two-step process. TiO_2 nanoparticles with homogeneous dispersion on the SBA-15 silica were treated with urea to form nitrogen-doped TiO_2 -SBA-15 material. The absorption of visible light for the material comes from the partial substitution of the oxygen in TiO_2 by nitrogen atoms. The nitrogen-doped TiO_2 -SBA-15 material exhibits a good photocatalytic activity for the degradation of methylene blue in the aqueous solution under visible light.

Acknowledgment

The financial support from the National Foundation for Science and Technology Development of Vietnam (NAFOS-TED, 104.03.2011.11) is gratefully acknowledged.

References

- [1] T. L. Thompson and J. T. Yates Jr., "Surface science studies of the photoactivation of TiO_2 —New photochemical processes," *Chemical Reviews*, vol. 106, no. 10, pp. 4428–4453, 2006.
- [2] M. Ni, M. K. H. Leung, D. Y. C. Leung, and K. Sumathy, "A review and recent developments in photocatalytic water-splitting using TiO_2 for hydrogen production," *Renewable and Sustainable Energy Reviews*, vol. 11, no. 3, pp. 401–425, 2007.
- [3] Y.-H. Tseng, H.-Y. Lin, C.-S. Kuo, Y.-Y. Li, and C.-P. Huang, "Thermostability of nano- TiO_2 and its photocatalytic activity," *Reaction Kinetics and Catalysis Letters*, vol. 89, no. 1, pp. 63–69, 2006.
- [4] Y.-M. Lin, Y.-H. Tseng, J.-H. Huang, C. C. Chao, C.-C. Chen, and I. Wang, "Photocatalytic activity for degradation of nitrogen oxides over visible light responsive titania-based photocatalysts," *Environmental Science and Technology*, vol. 40, no. 5, pp. 1616–1621, 2006.
- [5] H. H. Tseng, W. W. Lee, M. C. Wei, B. S. Huang, M. C. Hsieh, and P. Y. Cheng, "Synthesis of TiO_2 /SBA-15 photocatalyst for the azo dye decolorization through the polyol method," *Chemical Engineering Journal*, vol. 210, pp. 529–538, 2012.
- [6] M. G. Sorolla, M. L. Dalida, P. Khemthong, and N. Grisdanurak, "Photocatalytic degradation of paraquat using nano-sized Cu-TiO_2 /SBA-15 under UV and visible light," *Journal of Environmental Sciences*, vol. 24, pp. 1125–1132, 2012.
- [7] S. Zhang, D. Jiang, T. Tang et al., " TiO_2 /SBA-15 photocatalysts synthesized through the surface acidolysis of $\text{Ti}(\text{O}^i\text{Bu})_4$ on carboxyl-modified SBA-15," *Catalysis Today*, vol. 158, no. 3–4, pp. 329–335, 2010.
- [8] T. Gao, G. Meng, Y. Tian, S. Sun, X. Liu, and L. Zhang, "Photoluminescence of ZnO nanoparticles loaded into porous anodic alumina hosts," *Journal of Physics Condensed Matter*, vol. 14, no. 47, pp. 12651–12656, 2002.

- [9] Y. Wang, H. Cheng, Y. Hao, J. Ma, W. Li, and S. Cai, "Photoelectrochemical properties of metal-ion-doped TiO₂ nanocrystalline electrodes," *Thin Solid Films*, vol. 349, no. 1, pp. 120–125, 1999.
- [10] H. Yamashita, M. Honda, M. Harada et al., "Preparation of titanium oxide photocatalysts anchored on porous silica glass by a metal ion-implantation method and their photocatalytic reactivities for the degradation of 2-propanol diluted in water," *Journal of Physical Chemistry B*, vol. 102, no. 52, pp. 10707–10711, 1998.
- [11] R. Asahi, T. Morikawa, T. Ohwaki, K. Aoki, and Y. Taga, "Visible-light photocatalysis in nitrogen-doped titanium oxides," *Science*, vol. 293, no. 5528, pp. 269–271, 2001.
- [12] T. Lindgren, J. M. Mwabora, E. Avandano et al., "Photoelectrochemical and optical properties of nitrogen doped titanium dioxide films prepared by reactive DC magnetron sputtering," *Journal of Physical Chemistry B*, vol. 107, no. 24, pp. 5709–5716, 2003.
- [13] H. Irie, Y. Watanabe, and K. Hashimoto, "Nitrogen-concentration dependence on photocatalytic activity of TiO_{2-x}N_x powders," *Journal of Physical Chemistry B*, vol. 107, no. 23, pp. 5483–5486, 2003.
- [14] O. Diwald, T. L. Thompson, T. Zubkov, E. G. Goralski, S. D. Walck, and J. T. Yates Jr., "Photochemical activity of nitrogen-doped rutile TiO₂(110) in visible light," *Journal of Physical Chemistry B*, vol. 108, no. 19, pp. 6004–6008, 2004.
- [15] C. Burda, Y. Lou, X. Chen, A. C. S. Samia, J. Stout, and J. L. Gole, "Enhanced nitrogen doping in TiO₂ nanoparticles," *Nano Letters*, vol. 3, no. 8, pp. 1049–1051, 2003.
- [16] J. L. Gole, J. D. Stout, C. Burda, Y. Lou, and X. Chen, "Highly efficient formation of visible light tunable TiO_{2-x}N_x photocatalysts and their transformation at the nanoscale," *Journal of Physical Chemistry B*, vol. 108, no. 4, pp. 1230–1240, 2004.
- [17] Y. Cong, J. Zhang, F. Chen, and M. Anpo, "Synthesis and characterization of nitrogen-doped TiO₂ nanophotocatalyst with high visible light activity," *Journal of Physical Chemistry C*, vol. 111, no. 19, pp. 6976–6982, 2007.
- [18] S. Sakthivel, M. Janczarek, and H. Kisch, "Visible light activity and photoelectrochemical properties of nitrogen-doped TiO₂," *Journal of Physical Chemistry B*, vol. 108, no. 50, pp. 19384–19387, 2004.
- [19] M. Xing, J. Zhang, and F. Chen, "New approaches to prepare nitrogen-doped TiO₂ photocatalysts and study on their photocatalytic activities in visible light," *Applied Catalysis B*, vol. 89, no. 3–4, pp. 563–569, 2009.
- [20] R. Nakamura, T. Tanaka, and Y. Nakato, "Mechanism for visible light responses in anodic photocurrents at N-doped TiO₂ film electrodes," *Journal of Physical Chemistry B*, vol. 108, no. 30, pp. 10617–10620, 2004.
- [21] M. Kitano, K. Funatsu, M. Matsuoka, M. Ueshima, and M. Anpo, "Preparation of nitrogen-substituted TiO₂ thin film photocatalysts by the radio frequency magnetron sputtering deposition method and their photocatalytic reactivity under visible light irradiation," *Journal of Physical Chemistry B*, vol. 110, no. 50, pp. 25266–25272, 2006.
- [22] M. Maeda and T. Watanabe, "Visible light photocatalysis of nitrogen-doped titanium oxide films prepared by plasma-enhanced chemical vapor deposition," *Journal of the Electrochemical Society*, vol. 153, no. 3, pp. C186–C189, 2006.
- [23] M. Batzill, E. H. Morales, and U. Diebold, "Influence of nitrogen doping on the defect formation and surface properties of TiO₂ rutile and anatase," *Physical Review Letters*, vol. 96, no. 2, Article ID 26103, 4 pages, 2006.
- [24] C. Di Valentin, G. Pacchioni, A. Selloni, S. Livraghi, and E. Giamello, "Characterization of paramagnetic species in N-doped TiO₂ powders by EPR spectroscopy and DFT calculations," *Journal of Physical Chemistry B*, vol. 109, no. 23, pp. 11414–11419, 2005.
- [25] T. Ihara, M. Miyoshi, Y. Iriyama, O. Matsumoto, and S. Sugihara, "Visible-light-active titanium oxide photocatalyst realized by an oxygen-deficient structure and by nitrogen doping," *Applied Catalysis B*, vol. 42, no. 4, pp. 403–409, 2003.
- [26] S. U. M. Khan, M. Al-Shahry, and W. B. Ingler Jr., "Efficient photochemical water splitting by a chemically modified n-TiO₂," *Science*, vol. 297, no. 5590, pp. 2243–2245, 2002.
- [27] S. Sakthivel and H. Kisch, "Daylight photocatalysis by carbon-modified titanium dioxide," *Angewandte Chemie*, vol. 42, no. 40, pp. 4908–4911, 2003.
- [28] H. Irie, Y. Watanabe, and K. Hashimoto, "Carbon-doped anatase TiO₂ powders as a visible-light sensitive photocatalyst," *Chemistry Letters*, vol. 32, no. 8, pp. 772–773, 2003.
- [29] M. Shen, Z. Wu, H. Huang, Y. Du, Z. Zou, and P. Yang, "Carbon-doped anatase TiO₂ obtained from TiC for photocatalysis under visible light irradiation," *Materials Letters*, vol. 60, no. 5, pp. 693–697, 2006.
- [30] S.-C. Moon, H. Mametsuka, S. Tabata, and E. Suzuki, "Photocatalytic production of hydrogen from water using TiO₂ and B/TiO₂," *Catalysis Today*, vol. 58, no. 2, pp. 125–132, 2000.
- [31] W. Zhao, W. Ma, C. Chen, J. Zhao, and Z. Shuai, "Efficient Degradation of Toxic Organic Pollutants with Ni₂O₃/TiO_{2-x}B_x under Visible Irradiation," *Journal of the American Chemical Society*, vol. 126, no. 15, pp. 4782–4783, 2004.
- [32] D. Chen, D. Yang, Q. Wang, and Z. Jiang, "Effects of boron doping on photocatalytic activity and microstructure of titanium dioxide nanoparticles," *Industrial and Engineering Chemistry Research*, vol. 45, no. 12, pp. 4110–4116, 2006.
- [33] A. Zaleska, J. W. Sobczak, E. Grabowska, and J. Hupka, "Preparation and photocatalytic activity of boron-modified TiO₂ under UV and visible light," *Applied Catalysis B*, vol. 78, no. 1–2, pp. 92–100, 2008.
- [34] T. Ohno, T. Mitsui, and M. Matsumura, "Photocatalytic activity of S-doped TiO₂ photocatalyst under visible light," *Chemistry Letters*, vol. 32, no. 4, pp. 364–365, 2003.
- [35] T. Ohno, M. Akiyoshi, T. Umabayashi, K. Asai, T. Mitsui, and M. Matsumura, "Preparation of S-doped TiO₂ photocatalysts and their photocatalytic activities under visible light," *Applied Catalysis A*, vol. 265, no. 1, pp. 115–121, 2004.
- [36] T. Umabayashi, T. Yamaki, H. Itoh, and K. Asai, "Band gap narrowing of titanium dioxide by sulfur doping," *Applied Physics Letters*, vol. 81, no. 3, pp. 454–456, 2002.
- [37] T. Umabayashi, T. Yamaki, S. Yamamoto et al., "Sulfur-doping of rutile-titanium dioxide by ion implantation: photocurrent spectroscopy and first-principles band calculation studies," *Journal of Applied Physics*, vol. 93, no. 9, pp. 5156–5160, 2003.
- [38] L. Lin, R. Y. Zheng, J. L. Xie, Y. X. Zhu, and Y. C. Xie, "Synthesis and characterization of phosphor and nitrogen co-doped titania," *Applied Catalysis B*, vol. 76, no. 1–2, pp. 196–202, 2007.
- [39] J. C. Yu, J. Yu, W. Ho, Z. Jiang, and L. Zhang, "Effects of F-doping on the photocatalytic activity and microstructures of nanocrystalline TiO₂ powders," *Chemistry of Materials*, vol. 14, no. 9, pp. 3808–3816, 2002.

- [40] J.-G. Yu, J. C. Yu, B. Cheng, S. K. Hark, and K. Iu, "The effect of F⁻-doping and temperature on the structural and textural evolution of mesoporous TiO₂ powders," *Journal of Solid State Chemistry*, vol. 174, no. 2, pp. 372–380, 2003.
- [41] G. Liu, Z. Chen, C. Dong et al., "Visible light photocatalyst: iodine-doped mesoporous titania with a bicrystalline framework," *Journal of Physical Chemistry B*, vol. 110, no. 42, pp. 20823–20828, 2006.
- [42] S. Tojo, T. Tachikawa, M. Fujitsuka, and T. Majima, "Iodine-doped TiO₂ photocatalysts: correlation between band structure and mechanism," *Journal of Physical Chemistry C*, vol. 112, no. 38, pp. 14948–14954, 2008.
- [43] J. Ananpattarachai, P. Kajitvichyanukul, and S. Seraphin, "Visible light absorption ability and photocatalytic oxidation activity of various interstitial N-doped TiO₂ prepared from different nitrogen dopants," *Journal of Hazardous Materials*, vol. 168, no. 1, pp. 253–261, 2009.
- [44] S. Zhou, J. Lv, L. K. Guo et al., "Preparation and photocatalytic properties of N-doped nano-TiO₂/muscovite composites," *Applied Surface Science*, vol. 258, no. 16, pp. 6136–6141, 2012.
- [45] C. C. Hu, T. C. Hsu, and S. Y. Lu, "Effect of nitrogen doping on the microstructure and visible light photocatalysis of titanate nanotubes by a facile cohydrothermal synthesis via urea treatment," *Applied Surface Science*, pp. 171–178, 2013.
- [46] D. Zhao, J. Feng, Q. Huo et al., "Triblock copolymer syntheses of mesoporous silica with periodic 50 to 300 angstrom pores," *Science*, vol. 279, no. 5350, pp. 548–552, 1998.
- [47] X. Wang, K. S. K. Lin, J. C. C. Chan, and S. Cheng, "Direct synthesis and catalytic applications of ordered large pore aminopropyl-functionalized SBA-15 mesoporous materials," *Journal of Physical Chemistry B*, vol. 109, no. 5, pp. 1763–1769, 2005.
- [48] L. Mercier and T. J. Pinnavaia, "Direct synthesis of hybrid organic-inorganic nanoporous silica by a neutral amine assembly route: structure-function control by stoichiometric incorporation of organosiloxane molecules," *Chemistry of Materials*, vol. 12, no. 1, pp. 188–196, 2000.
- [49] Y. Cong, J. Zhang, F. Chen, and M. Anpo, "Synthesis and characterization of nitrogen-doped TiO₂ nanophotocatalyst with high visible light activity," *Journal of Physical Chemistry C*, vol. 111, no. 19, pp. 6976–6982, 2007.
- [50] M. Sathish, B. Viswanathan, R. P. Viswanath, and C. S. Gopinath, "Synthesis, characterization, electronic structure, and photocatalytic activity of nitrogen-doped TiO₂ nanocatalyst," *Chemistry of Materials*, vol. 17, no. 25, pp. 6349–6353, 2005.
- [51] M. Xing, J. Zhang, and F. Chen, "New approaches to prepare nitrogen-doped TiO₂ photocatalysts and study on their photocatalytic activities in visible light," *Applied Catalysis B*, vol. 89, no. 3-4, pp. 563–569, 2009.
- [52] D. Wu, M. Long, W. Cai, C. Chen, and Y. Wu, "Low temperature hydrothermal synthesis of N-doped TiO₂ photocatalyst with high visible-light activity," *Journal of Alloys and Compounds*, vol. 502, no. 2, pp. 289–294, 2010.
- [53] H. Wang, J. Yan, W. Chang, and Z. Zhang, "Practical synthesis of aromatic amines by photocatalytic reduction of aromatic nitro compounds on nanoparticles N-doped TiO₂," *Catalysis Communications*, vol. 10, no. 6, pp. 989–994, 2009.
- [54] M. Sathish, B. Viswanathan, R. P. Viswanath, and C. S. Gopinath, "Synthesis, characterization, electronic structure, and photocatalytic activity of nitrogen-doped TiO₂ nanocatalyst," *Chemistry of Materials*, vol. 17, no. 25, pp. 6349–6353, 2005.



Hindawi

Submit your manuscripts at
<http://www.hindawi.com>

